

# Metamaterials and Metasurfaces: Contemporary Approaches in Antenna Design

Krunal Patel<sup>1</sup>, Dr. Kushal Tuckley<sup>2</sup>, Dr. Joshi M.<sup>3</sup>

<sup>1</sup>*Ph.D. Student*

<sup>3</sup>*Assistant Professor*  
MPSTME, NMIMS UNIVERSITY,

MUMBAI, MAHARASHTRA.

<sup>2</sup>*Adjunct Professor*

INDIAN INSTITUTE OF TECHNOLOGY, BOMBAY

(E-mail: [krunalmailbox@rediffmail.com](mailto:krunalmailbox@rediffmail.com))

**Abstract**— Metamaterials are artificial structures that have substantial proficiency of manipulating the properties of the incident electromagnetic wave. They are designed to exhibit unusual Electromagnetic properties like negative permittivity and permeability. The unit cells contain metallic resonators which interact with electromagnetic wave and modify the properties of the incident electromagnetic wave. Metamaterials are built from periodically arranged unit cells. Metamaterials have become a remarkable research area and have a wide range of exceptional applications in Electromagnetics including cavity resonators, absorbers, terahertz switches etc. From a general context, metasurfaces are designed to manipulate the polarization, the phase, and the amplitude of electromagnetic fields. A rich heterogeneity of metasurface applications has been observed in the literature hitherto. In this paper, the review of the principles and operation of artificial composite structure is presented. In addition, simulations of various types of metasurface loaded patch antennas are carried out and their applications are explained. The simulation results show the importance of MoM based software in design and analysis of metasurface loaded patch antenna.

**Keywords**— HFSS, CST Microwave Studio, EBGs, Metasurfaces, Metamaterials.

## INTRODUCTION

Periodic structures are used in a variety of applications like Airborne Radomes, Band-Reject Filters, Subreflectors and Main Reflectors with Dichroic Structures, Circuit Analog Absorbers and Meanderline Polarizers [14]. Hybrid Radomes were designed to reduce the Radar Cross Section [16] of antennas outside their operating band. With the help of Frequency Selective Surfaces, planar and non-planar antennas can be designed to be imperceptible in the backscatter direction over a wider bandwidth. Antennas mounted on masts can be covered by Frequency Selective Surface to deflect out of band incident plane waves. A dual

reflector Cassegrainian system has the hyperboloid made of a dichroic structure which is a periodic structure allows one frequency band and rejects the other frequency band. Periodic structures can be made of lossy material but at the time can be very useful. Lossy periodic structures are used in Circuit Analog Absorbers. Such periodic structure consist of crossed elements made of a resistive material backed by a ground plane. Using meanderline polarizers an incident wave tilted at 45 degree may be decomposed into vertical and horizontal components where the vertical component is delayed and the horizontal component is advanced. If a dielectric structure is added next to a periodic structure, the resonant frequency changes. A stratified dielectric medium shifts the resonant frequency. It can also change the shape and the angle of incidence variation of the resonant curves. The progress in metamaterials can be counted from the classic paper of Pendry in which he presented an arduous goal of creating artificial medium with both negative permittivity and permeability in the same frequency band. The analysis of metamaterials deals with the effects that arise due to the real part of electric permittivity and magnetic permeability which can be manipulated to be negative to form a material with a negative refractive index. However, the imaginary part of the electric permittivity and magnetic permeability can also be manipulated to obtain unusual properties.

In particular, the electric permittivity and magnetic permeability of metamaterials can be influenced to develop very strong absorbers. By manipulating the electric permittivity and magnetic permeability, a metamaterial can be impedance-matched to free space and reflectivity can be minimized. By manipulating electric and magnetic resonances independently, it is possible to effectively absorb radiation through the electric and magnetic field components.

## 2. LEFT HANDED MATERIALS

It is appropriate to consider the classification of materials as shown in figure 1. All isotropic materials have positive values of permittivity and permeability. They are known as

DPS materials. Materials with negative  $\epsilon$  or  $\mu$  are termed as single negative materials and they are divided into materials with negative permittivity and negative permeability. Materials with simultaneously negative values of  $\epsilon$  and  $\mu$  are known as DNG materials.

through the boundary between left handed and right handed media. As shown in figure, the refraction of light occurs on the same side of the normal as the incident beam in case of DNG media whereas it occurs on the opposite side of the normal in case of DPS media. Thus double negative medium exhibits a negative refractive index.

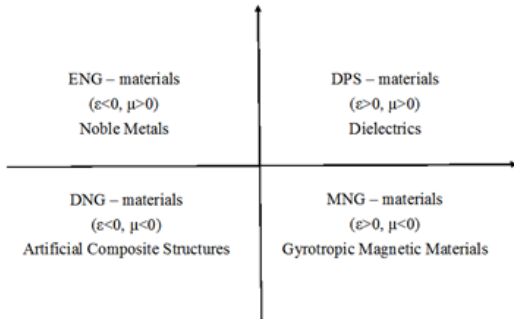


Figure 1. Classification of physical materials

From Faraday's Law and Ampere's Law,

$$\nabla \times \mathbf{E} = -\mu_0 \mu_R \frac{\partial \mathbf{H}}{\partial t} \quad (1)$$

$$\nabla \times \mathbf{H} = -\epsilon_0 \epsilon_R \frac{\partial \mathbf{E}}{\partial t} \quad (2)$$

The wave equation can be written as,

$$\nabla^2 \mathbf{E} = -\epsilon_0 \epsilon_R \mu_0 \mu_R \frac{\partial^2 \mathbf{E}}{\partial t^2} \quad (3)$$

Considering a time-harmonic and plane-wave variation for fields in Maxwell's Equations,

$$\mathbf{E}(x, y, z, t) = \mathbf{E} e^{i\omega t - i\mathbf{k} \cdot \mathbf{r}} \quad (4)$$

Where  $\mathbf{k}$  = wave vector

Similar expression can be applied to magnetic field intensity.

Then Maxwell's equations take the form,

$$\mathbf{k} \times \mathbf{E} = -\omega \mu_0 \mu_R \mathbf{H} \quad (5)$$

$$\mathbf{k} \times \mathbf{H} = \omega \epsilon_0 \epsilon_R \mathbf{E} \quad (6)$$

From the above equations, it can be observed that for Positive values of relative permittivity and permeability, the direction of wave propagation is governed by the right-hand rule. If these values are negative, then they form a left-handed system [1].

If the angle of refraction is observed, then an important difference between regular dielectrics and left-handed metamaterial can be realized when a wave is propagating

The Drude Model characterizes the metals at the optical frequencies by the relationship [18],

$$\epsilon(\omega) = \epsilon_0 \left[ 1 - \frac{\omega_p^2}{\omega(\omega + i\gamma)} \right] \quad (7)$$

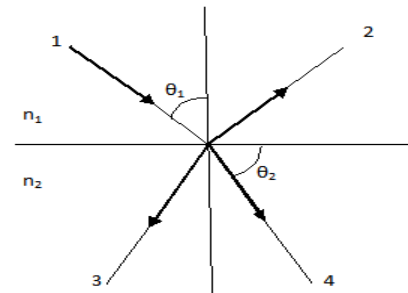


Figure 2. Reflection and refraction at the interface between DNG and DPS media

Where

$$\omega_p^2 = \frac{Ne^2}{m\epsilon_0} \quad (8)$$

$\omega_p^2$  is the plasma frequency. It represents the frequency with which the collection of free electrons oscillates in the presence of an external field.  $N$  represents the electron density,  $e$  and  $m$  represent the charge and mass respectively. The rate with which the amplitude of the plasma oscillation decreases is represented by  $\gamma$ . When  $\gamma=0$  and  $\omega < \omega_p$ , the medium is characterized by negative permittivity.

*Epsilon-negative Materials*

The first Epsilon Negative Structure was consisting of thin metal wires. Array of parallel thin metal wires which are infinitely long can be inserted in a dielectric medium. For such type of Epsilon-negative Materials, the effective permittivity can be written as [10],

$$\epsilon_{eff} = 1 - \frac{\omega_p^2}{\omega \left[ \omega - i \left( \frac{\omega_p^2 \alpha^2 \epsilon_0}{\sigma \pi r^2} \right) \right]} \quad (9)$$

Where  $r$  is the radius of individual wire,  $a$  is the period between the wires with  $r \ll a$ .  $\sigma$  represents the electrical conductivity.

*Mu-negative Materials*

The extensively analyzed Mu-negative structure is split-ring resonator (SRR). SRRs can have round or square shape. For

a circular double split ring resonator in vacuum, with a negligible thickness, effective permeability can be determined by [10],

$$\mu_{eff} = 1 - \frac{\frac{\pi r^2}{a}}{1 + \frac{2\sigma i}{\omega r \mu_0} - \frac{3d}{\pi^2 \mu_0 \omega^2 \epsilon_0 \epsilon_r^3}} \quad (10)$$

Where  $a$ =length of the unit cell,  $d$ =interval between the rings,  $r$ =the radius of the inner ring and  $\sigma$  is the electrical conductance.  $\Omega$  shaped structures offer substantially disparate properties in comparison with conventional SRR materials. The resonant frequency is directly dependent on the electric field orientation on the structure plane. Omega shaped structures are the most suitable for antennas, absorbing devices and lenses.

### PBG Materials

Properly designed photonic crystals have the capability of prohibiting the electromagnetic wave propagation. They can allow the wave propagation only along defined directions. Such artificially fabricated structures which can control the propagation of electromagnetic waves are called as Photonic Bandgap Materials. They are widely used in integrated circuits, microwave filters with sharp selectivity and navigational antennas.

A few comments are required on a) the differences between a metamaterial and a conventional Photonic Bandgap structure and b) the differences between a metasurface and a conventional Frequency Selective Surface. The behavior of a composite material can be subdivided into three regions, with distinctive behaviors in each region. Region 1 corresponds to the quasi-static region. This includes the frequencies at which the wavelength is much larger than the period of the structure. In this region classical mixing formulas are used to obtain equivalent permittivity and permeability. Region 2 applies to a region where the period of the structure is still small compared to a wavelength but the individual scatterers are designed in such a way that they can resonate. In this case a new class of material is realized, making possible the properties not found in nature. These scatterers are classified as double negative or near zero index materials and they are called metamaterials. When the wavelength becomes comparable to or smaller than the period of the structure, the composite can not behave as an effective medium. This corresponds to the third region in figure 3[17].

Full-wave approaches must be used to analyze the field interaction with the periodic structure. In this region higher order Floquet-Bloch modes must be considered.

These modes can interfere with the wave propagating through the structure which is known as a photonic bandgap or electromagnetic bandgap structure in this frequency range. These materials cannot be identified as metamaterials

or metasurfaces. At certain frequencies, these structures block the propagation of EM waves through the material. The frequency bands where it occurs are called as stop bands. At other frequencies, the periodic structure allows the wave to propagate and this range of frequencies is referred to as pass bands.

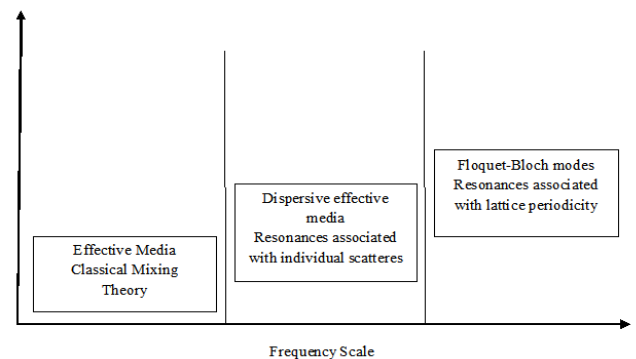


Figure 3. Three characteristic regions of a composite material

### Double Negative Materials

Design of metamaterials with negative refractive index can be categorized into the following structures[10].

- Thin wires & Split Ring Resonators
- Transmission lines
- Mushroom shaped structures

The classic structure is the combination of split ring resonators[2] and thin metal wires. Negative refractive index can be discerned in a very narrow frequency band owing to the resonance property of the unit cell. Revamped designs of resonators and metasoloids can be used to partially expand the frequency range.

### 3. TYPES OF METASURFACES

Various types of Metasurfaces have been investigated and designed to obtain the required parameters. Polarization Conversion Metamaterial works on the principle of Phase Cancellation. It leads to broadband performance. Concentric Rings are used to reduce out of band radar cross section. Artificial Magnetic Conductor reduces backscattering. Slotted Electromagnetic Bandgap Structures and Partially Reflecting Surface are used for gain enhancement. Tunable Fabri-Parot cavity can be used for dynamic tuning of frequency range. Resistor loaded crossed dipoles and ECLR structures result in broadband performance. Dipole array with Frequency Selective Surfaces can be used for out of band radar cross section reduction.

Metafilm consists of an array of isolated scatterers. Surfaces which have 'fishnet' type of structures are known as metascreens. These can be characterized by periodically spaced slots. A grating of parallel wires behaves like a metafilm in the direction normal to the axes of the wires. It will behave like a metascreen in the direction along the axes of the parallel wires.



Figure 4. A Metafilm

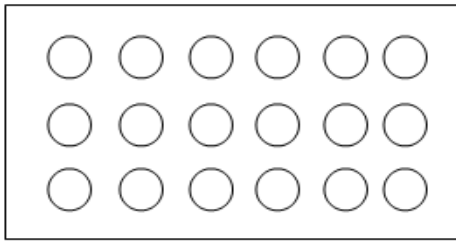


Figure 5. A Metascreen

The  $\lambda/2$  limit on the size of a resonant structure can be reduced if the cavity is partially filled with a metamaterial. The same thing can be accomplished with the help of a metasurface. The superiority of a metasurface is that it requires less physical volume than a three-dimensional metamaterial and it can be easily integrated with an antenna system.

4. PARAMETER EXTRACTION AND SIMULATION TECHNIQUES

The square split-ring resonator is selected to study the parameter extraction process of a metasurface. Let  $l_1$  and  $l_2$  be the lengths of the outer loop and inner loop respectively. In simulation  $l_1=2.2$  mm and  $l_2=1.5$  mm are chosen. The split gap is 0.3 mm. The width of the ring is 0.2 mm. Spacing between the two rings is 0.15 mm and a microstrip line of width 0.14 mm is used as CRLH line on the bottom layer. The FR-4 substrate with 0.25 mm thickness and dielectric constant of 4.4 is used to design the unit cell. The PEC and PMC periodic boundary conditions approach is followed for parameter extraction. In addition to these boundaries HFSS provides master-slave boundaries to realize periodic structures. The boundary conditions at the master are enforced at the slave's surface to obtain periodicity of the unit cell. These boundary conditions can also simulate complex polygon-shaped structures. The "Waveport" excitation is used to excite the structure. However, to simulate obliquely incident waves "Floquet Port" approach is better. It can only be used with master-slave boundary conditions. In this approach the S parameters are extracted based on the dominant mode. For parameter extraction the time reversal property of the Fourier Transform should be applied taking into account the time factor assumptions in HFSS. From the values of S-parameters real and imaginary values of permittivity and permeability can be calculated [4]. Following the same approach real and imaginary values of refractive index can be calculated. The simulation results show the resonant frequency of 9 GHz approximately and it shows both the negative permittivity and permeability in the range of 8.8 GHz to 9.4 GHz. It shows double negative characteristics.

The refractive index and wave impedance can be calculated using the following equations.

$$n = \frac{1}{kd} \cos^{-1} \left[ \frac{1}{2S_{21}} (1 - S_{11}^2 + S_{21}^2) \right] \tag{11}$$

$$z = \sqrt{\frac{(1 + S_{11})^2 - S_{21}^2}{(1 - S_{11})^2 - S_{21}^2}} \tag{12}$$

The effective permittivity can be calculated as,

$$\epsilon = \frac{n}{z} \tag{13}$$

The effective permeability can be calculated as,

$$\mu = nz \tag{14}$$

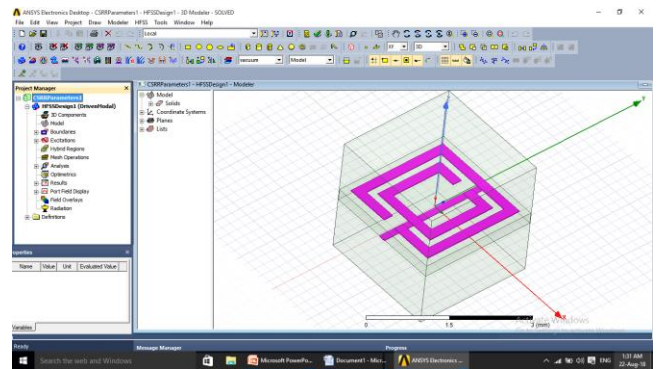


Figure 6. The simulation model of SRR-DGS Unit Cell (HFSS)

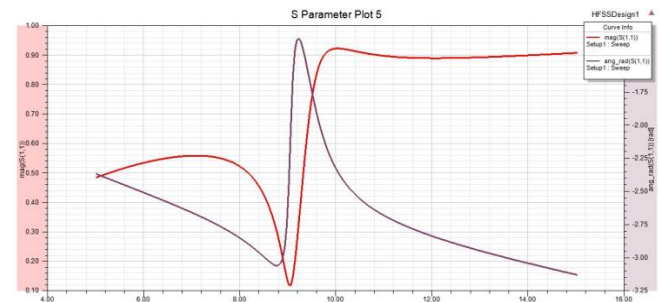


Figure 7. Magnitude and Phase of Reflection Parameter

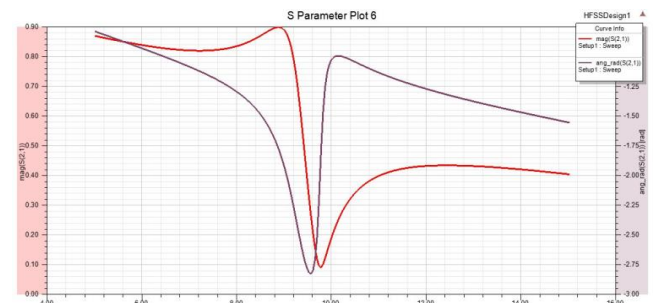


Figure 8. Magnitude and Phase of Transmission Parameters

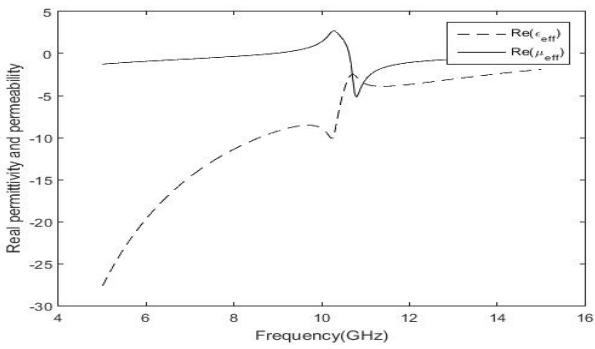


Figure 9. The real values of Epsilon and Mu

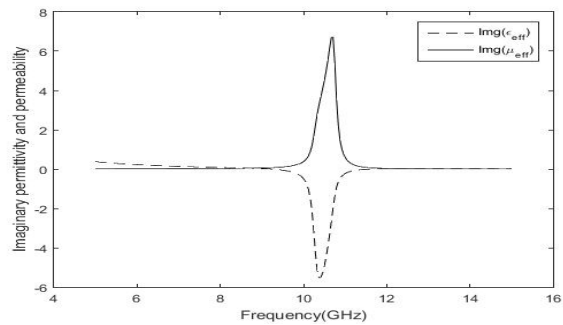


Figure 10. The imaginary values of Epsilon and Mu

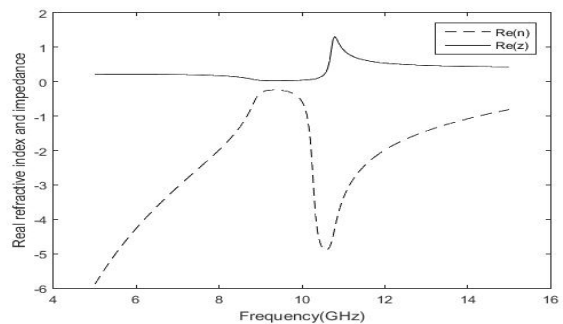


Figure 11. The real values of refractive index and impedance

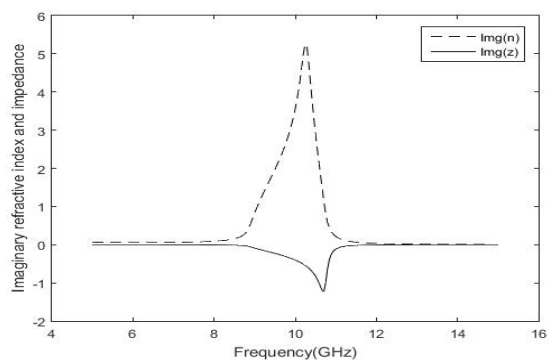


Figure 12. The imaginary values of refractive index and impedance

4.1 Equivalent Circuit Modeling of an SRR cell

The right-handed transmission line (RHTL) is realized by two series inductors and a shunt capacitor. The split ring resonator forms a parallel resonant circuit. If SRR is etched in the ground plane, a parallel resonant circuit is added to the equivalent RHTL. The transmission zero location is determined by the resonant frequency of the shunt circuit.

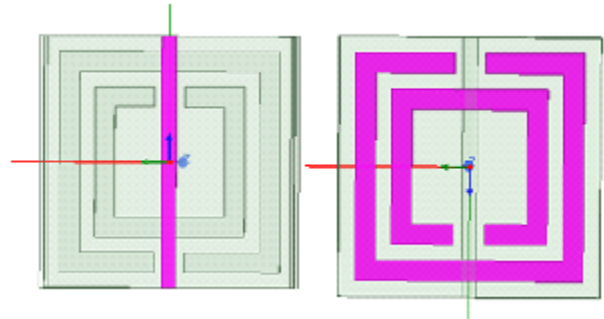


Figure 13. The CRLH line and SRR structure

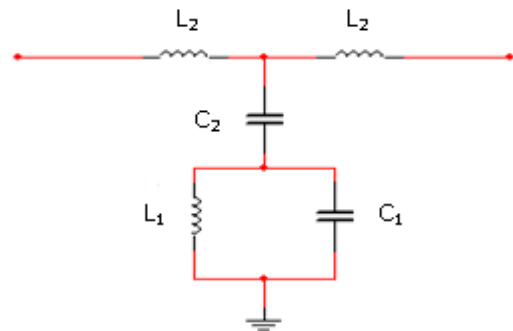


Figure 14. Equivalent circuit of an SRR DGS Unit Cell

Considering the admittances of shunt branches, the impedance of parallel resonant circuit can be written as,

$$Z_1 = \frac{1}{j\omega C_1 + \frac{1}{j\omega L_1}} \tag{15}$$

The impedance of capacitor C<sub>2</sub> is expressed as,

$$Z_2 = \frac{1}{j\omega C_2} \tag{16}$$

The transmission null is obtained as,

$$Z_1 + Z_2 = 0 \tag{17}$$

The resonant frequency can be calculated as,

$$f_s = \frac{1}{2\pi\sqrt{L_1(C_1 + C_2)}} \tag{18}$$

The following figures show parametric analysis of Split Ring Resonator.

If the side length of the Split Ring Resonator is increased, the value of L<sub>1</sub> increases, the cutoff frequency is reduced. If the split gap increases, the value of capacitance C<sub>1</sub> decreases

so that the transmission null is obtained at a higher frequency.

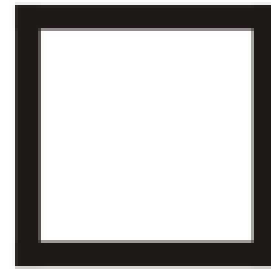


Figure 18. Square ring structure for wideband RCS reduction

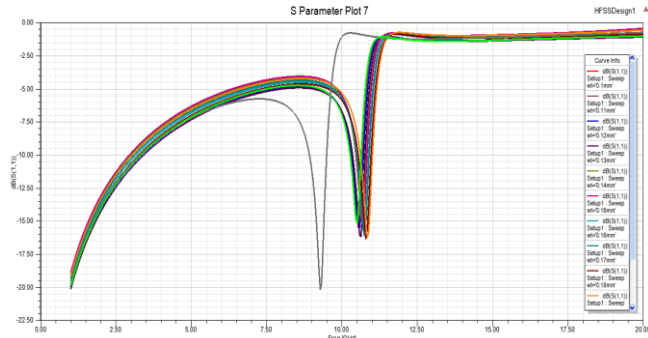


Figure 15. Variation of return loss with respect to width of the ring (Ansys HFSS)

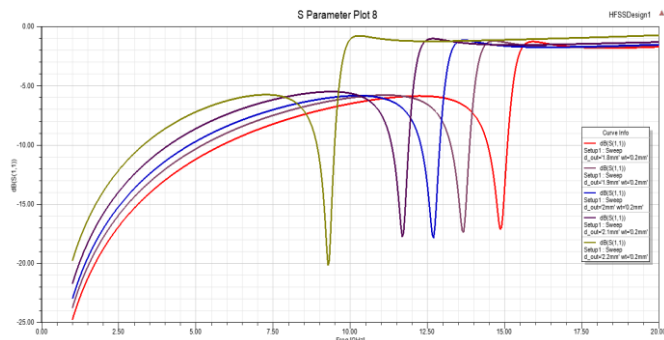


Figure 16. Variation of return loss with respect to the length of the outer ring (Ansys HFSS)

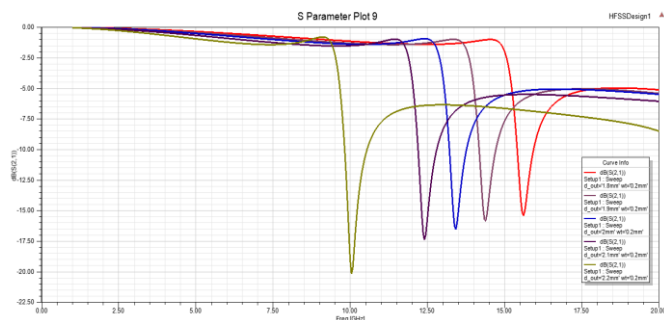


Figure 17. Variation of  $S_{21}$  with respect to the length of the outer ring (Ansys HFSS)

5. RECENT DEVELOPMENTS IN THE AREA.

5.1 Square Rings for ultra wideband RCS reduction

Square rings with different array elements are used to reduce ultra wideband RCS. Square rings are simple to design and fabrication of the structure is easy. The dimensions of the structure are optimized to get the required Reflection Phase characteristics say 180 deg. ± 37 deg. etc.

5.2 Artificial Magnetic Conductors

When AMC structures combined with Perfect Electric Conductor structures and the former are arranged in checkerboard pattern, a phase difference of 180 deg. between the reflected fields can be observed because of destructive interference. They exhibit broadband performance. Fractional bandwidth of the order of 83% can be obtained with such type of structures. To achieve broadband performance, single band and dual band structures can be combined. As shown in figure, circular structure is used for single band performance, while square structure is used for multiband performance. With the help of such structure, the phase difference of (180±37) deg. can be achieved.

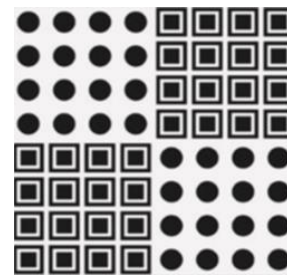


Figure 19. Broadband Checkerboard Metasurface

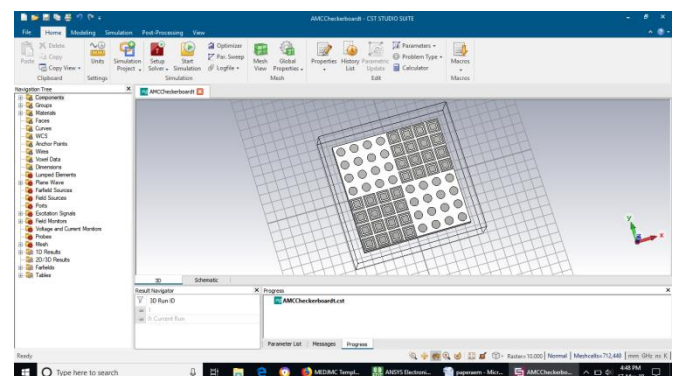


Figure 20. Simulation of AMC Checkerboard Metasurface

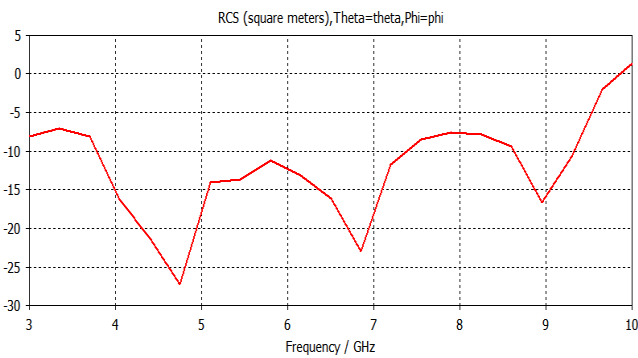


Figure 21. Monostatic RCS Graph

5.3 Fractal Geometries

With the help of fractal geometries, electrically large contours can be obtained. Because of this feature, resonant frequency can be reduced. Fractal geometries can be used for miniaturization of antenna because of the space filling properties. They can also be used to reduce the radar cross section of antenna. For example, instead of using circular loop antenna, a Koch island can be used to obtain increases input impedance. The star fractal geometry can be used to achieve multiband performance and backscattering reduction.

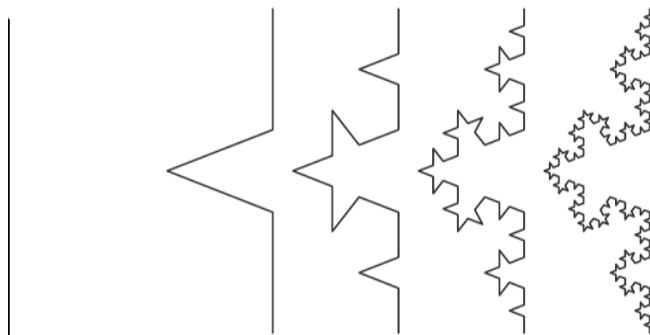


Figure 22. Example of a Koch Fractal Antenna

The triband performance of a star-shaped fractal antenna can be verified from the simulation results shown in the following figures.



Figure 23. Example of a fractal design

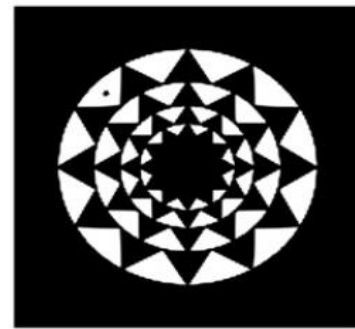


Figure 24. A star shaped fractal antenna

The star-shaped antenna is simulated with FR-4 substrate with dielectric constant of 4.3. It offers multiband performance because of its self symmetry property. If substrate height is increased then Monostatic RCS can be reduced.

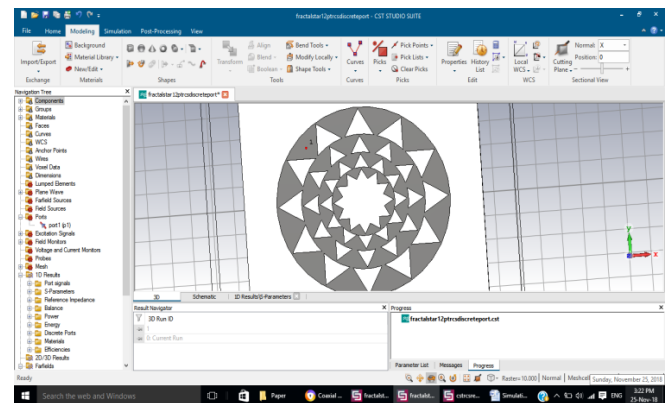


Figure 25. Simulation of a Star-shaped Fractal Antenna

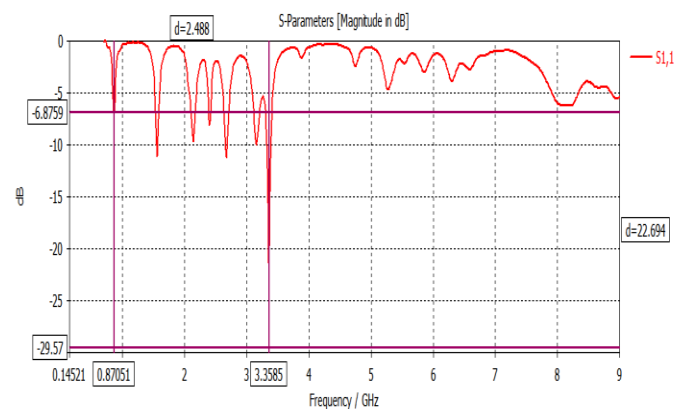


Figure 26. Simulated return loss parameter of the Star-shaped Fractal Antenna

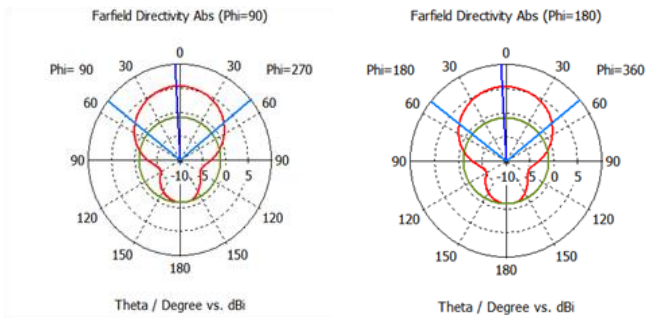


Figure 27. E-plane and H-plane Radiation Patterns of the Star shaped Fractal Antenna

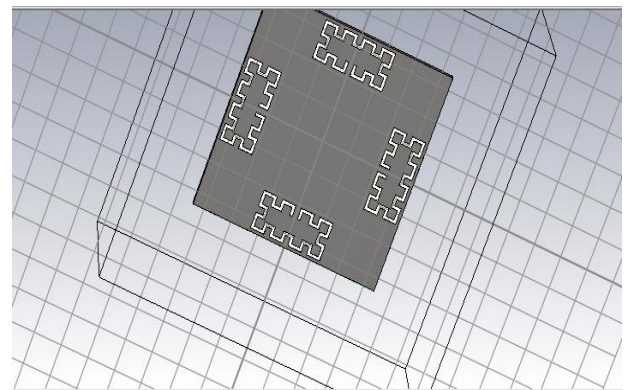


Figure 29. The combination of CSRR and Fractal Structure used in Microstrip Patch Antenna (CST Microwave Studio)

5.4 Polarization Conversion Metasurface

A combination of metasurface and fractal geometries can be used to design Polarization Conversion Metasurface. It gives wider bandwidth and improved polarization efficiency. When fractals are used with metamaterials and they are arranged in chessboard like pattern, there will be 180 deg. phase difference between the incident and the reflected waves and destructive interference can be observed. Hence the reflected wave cannot be detected by the receiving antenna. Figure shows an example of a quasi-fractal structure used to achieve backscatter reduction.



Figure 28. A Quasi-Fractal Structure

5.5. Combination of CSRR and Fractal Structure

CSRR exhibits unusual electromagnetic properties at resonant frequency when plane wave excitation is used. This feature of CSRR can be combined with Fractal structure to design novel structures. Figure shows the simulation of such a design which shows the combination of CSRR and Koch curves. Because of the space filling properties of the Koch curves, this design has longer slots as compared to conventional design. It will increase the equivalent capacitance. As the capacitance increases, the quality factor decreases and loss increases. This property is exploited to obtain Radar Cross Section reduction of the antenna.

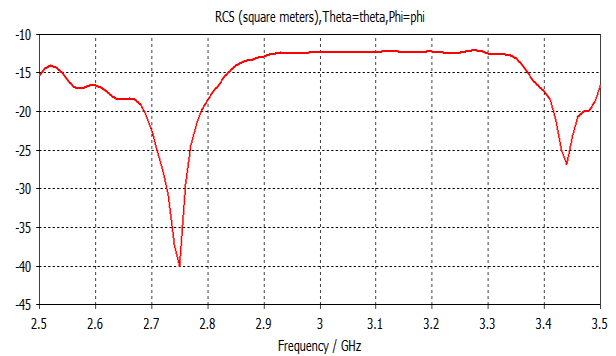


Figure 30. The RCS reduction graph

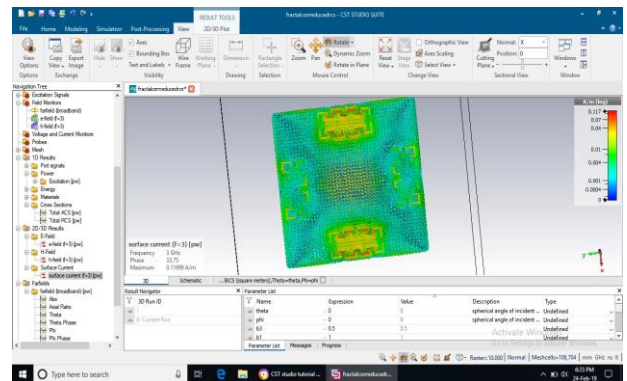


Figure 31. Current distribution on the CSRR with Fractals

The antenna is fabricated on F4B-2 substrate with operating frequency of 3.25 GHz. Because of its geometry the equivalent capacitance increases resulting higher loss.

5.6 Patch Antenna loaded with JC Structure

In the following figure, an array of Jerusalem-Cross structure is loaded below the patch antenna to achieve RCS reduction. This design also leads to miniaturization of patch antenna. In this design FR-4 substrate is used and the antenna with JC structure resonates at 2.4 GHz.

## 7. REFERENCES

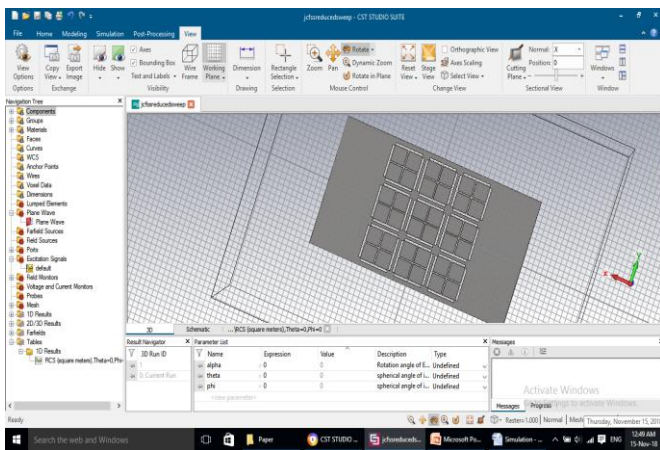


Figure 32. Patch antenna loaded with JC structure

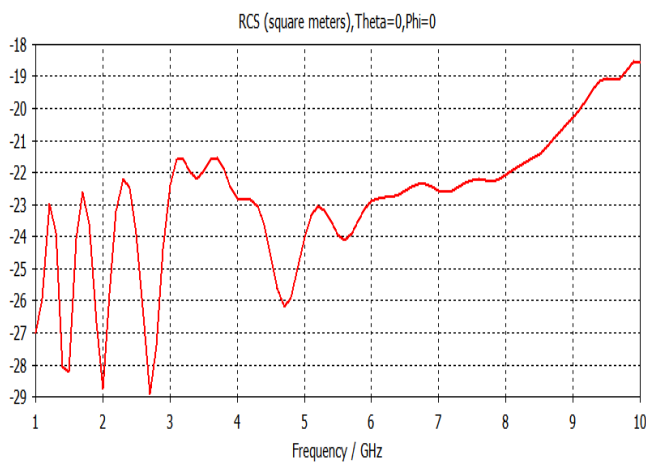


Figure 33. RCS characteristics of the patch antenna loaded with JC structure (CST Studio)

## 6. CONCLUSION

Metasurfaces are alternatives to bulk three dimensional metamaterials. Because of their two-dimensional structure, they require less physical space and can exhibit lower loss. They can be designed by placing scatterers in periodic or pseudo-periodic style. The concept of metasurface can also be stretched further to one-dimensional metamaterial. The performance of one-dimensional metasurfaces is substantially controlled by their density while two-dimensional metasurfaces rely on both the density and near-field coupling configuration of the metasurface. The potential of Frequency Selective Surfaces and metasurfaces has landscaped the areas of RF, Microwaves, Photonics and Optics. If equivalent circuit modeling is unavailable, then these simulation tools can be used for the prediction of antenna performance.

- [1] G. Minatti, F. Caminita, E. Martini, S. Maci, "Analysis and design of metasurface antennas", Loughborough Antennas & Propagation Conference (LAPC 2017).
- [2] Ji Liu, Yongjiu Zhao, Shengli Jia, "Fast design of multilayer cascade metasurface absorbers using particle swarm optimization", 2016 11th International Symposium on Antennas, Propagation and EM Theory (ISAPE), 2016.
- [3] Lina Qiu, Gaobiao Xiao, Xianghong Kong, "Broadband diffuse scattering metasurface with units of randomly distributed sizes", 2017 IEEE Electrical Design of Advanced Packaging and Systems Symposium (EDAPS), 2017.
- [4] Wenquan Cao, Yang Xiang, Bangning Zhang, Aijun Liu, Tongbin Yu, Daosheng Guo, "A Low-Cost Compact Patch Antenna With Beam Steering Based on CSRR-Loaded Ground" IEEE Antennas and Wireless Propagation Letters Volume 10, 1520 – 1523, 2011
- [5] Markos, P., C.M. Soukoulis, "Numerical studies of left-handed materials and arrays of split ring resonators," Journal of Applied Physics, Vol. 92, No. 5, 2929-2936, 2002.
- [6] Andrea Massa, Giacomo Oliveri, "Metasurface and metamaterial by design", 2014 International Radar Conference, 2014, pp. 1-5.
- [7] De Song Wang, Bao Jie Chen, Chi Hou Chan, "High-Selectivity Bandpass Frequency-Selective Surface in Terahertz Band", IEEE Transactions on Terahertz Science and Technology, vol. 6, no. 2, pp. 284-291, 2016.
- [8] Szabo Z., Park G. H., Hedge R. and Li E. -P. - A unique extraction of metamaterial parameters based on Kramers-Kronig relationship, IEEE Transactions on Microwave Theory & Techniques, 58 (10) (2010), 2646-2653.
- [9] D.R. Smith, D.C. Vier, Th. Koschny, C.M. Soukoulis, "Electromagnetic Parameter Retrieval from Inhomogeneous Metamaterials," Physics Review E, 71, 3, 2005, 036617.
- [10] I.A. Buriak, V.O. Zhurba, G.S. Vorobjov, V.R. Kulizhko, O.K. Kononov, Oleksandr Rybalko, "Metamaterials: Theory, Classification and Application Strategies (Review)", Journal of nano- and electronic physics, Vol. 8, No 4(2), 04088-1 to 04088-11, 2016.
- [11] N. Engheta, R.W. Ziolkowski, Metamaterials: Physics and Engineering Explorations, IEEE Wiley, New York, 2006.
- [12] Lee Y., Hao Y., "Characterization of microstrip patch antennas on metamaterial substrates loaded with complementary split ring resonators", Microwave Optical Technology Letters, 50 (8) (2008), pp. 2131-2135.
- [13] X. Chen, T.M. Grzegorzeczyk, B. Wu, J. Pancheco, Jr., and J.A.Kong, "Robust method to retrieve the constitutive effective parameters of metamaterials", Physics Review B, 65, 19, April 2002, 195104.

- [14] B.A. Munk, *Frequency Selective Surfaces: Theory and Design*, Wiley, New York, 2000.
- [15] Yongtao Jia, Ying Liu, Shuxi Gong, "RCS reduction of microstrip antenna by complementary split-ring resonators structure", 2014 International Workshop on Antenna Technology: Small Antennas, Novel EM Structures and Materials, and Applications (iWAT), 2014, pp. 336-339.
- [16] E.F. Knott, J.F. Shaeffer and M.T. Tuley, *Radar Cross Section*, 2<sup>nd</sup> ed., Sci. Tech Publishing, NC, 2004.
- [17] Christopher L. Holloway, E.F. Kuester, J.A. Gordon, John O'Hara, Jim Booth and D.R. Smith, "An overview of the Theory and Applications of Metasurfaces: The two-dimensional equivalents of Metamaterials", *IEEE Antennas and Propagation Magazine*, Vol. 54, No. 2, pp. 10-34, April 2012.
- [18] Marek S. Wartak, Kosmas L. Tsakmakidis and Ortwin Hess, "Introduction to Metamaterials", *Physics in Canada*, Vol. 67, No. 1, pp. 30-34, 2011.
- [19] T.J. Cui, W.X. Tang, X.M. Yang, Z.L. Mei and W.X. Jiang, "Metamaterials: Beyond Crystals, Noncrystals, and Quasicrystals, 1<sup>st</sup> Edition", Boca Raton: CRC Press 2016.
- [20] J.Y. Yin, X. Wan, Q. Zhang and T.J. Cui, "Ultra wideband polarization-selective conversions of electromagnetic waves by metasurface under large-range incident angles", *Sci. Rep.*, Vol. 5, Jul. 2015.
- [21] S. Tretyakov and S. Maslovski, "Thin Composite Radar Absorber Operational for All Incidence Angles," 33<sup>rd</sup> Eur. Microw. Conf., Munich, Germany, vol.3, pp.1107-1110, Oct, 2003.
- [22] S. Zouhdi, A. Sihvola, and M. Aarsalane, Eds., *Advances in Electromagnetic of Complex Media and Metamaterials*. Dordrecht, The Netherlands: Kluwer, 2002
- [23] X. Gao, X. Han, W.P. Cao, H.O. Li, H.F. Ma, T.J. Cui, "Ultrawideband and high-efficiency linear polarization converter based on double V-shaped metasurface", *IEEE Trans. Antennas Propag.*, vol. 63, no. 8, pp. 3522-3530, Aug. 2015.
- [24] S.H. Esmaeli, S.H. Sedighy, "Wideband radar cross section reduction by AMC", *Electron. Lett.*, vol. 52, pp. 70-71, Jan. 2016.
- [25] Y. Zhang et al., "Broadband diffuse terahertz wave scattering by flexible metasurface with randomized phase distribution", *Sci. Rep.*, vol. 6, pp. 26875, May 2016.
- [26] Kai, He, Zhang Jingling, and Lv Yinghua, "Design of dual band low-RCS coupling slot antenna based on AMC structure," *Environmental Electromagnetics (CEEM)*, 7th Asia-Pacific Conference on. IEEE, Hangzhou, 2015, pp. 44 – 46.
- [27] L.K. Sun, H.F. Cheng, Y.J. Zhou, J. Wang, "Broad band metamaterial absorber based on coupling resistive frequency selective surfaces", *Opt. Exp.*, vol. 20, pp. 4675-4680, 2012.
- [28] G.I. Kiani, A.R. Weily, K.P. Esselle, "A novel absorb/transmit FSS for secure indoor wireless network with reduced multipath fading", *IEEE Microw. Wireless Compon. Lett.*, vol. 16, no. 3, pp. 378-380, 2006.
- [29] Lu Lei, S. Qu, H. Ma, F. Yu, S. Xia, Z. Xu, P. Bai, "A polarization-independent wide-angle dual directional absorption metamaterial absorber", *Progress In Electromagnetic Research*, vol. 27, pp. 191-201, 2012.
- [30] Edalati, Kamal Sarabandi, "Wideband wide angle polarization independent RCS Reduction using nonabsorptive miniaturized-element frequency selective surfaces", *IEEE Trans. Antennas Propag.*, vol. 62, no. 2, pp. 747-754, 2014.